III European Conference on Computational Mechanics
Solids, Structures and Coupled Problems in Engineering
C.A. Mota Soares et.al. (eds.)
Lisbon, Portugal, 5-8 June 2006

NUMERICAL ANALYSIS OF PASSIVE EARTH PRESSURES WITH INTERFACES

Jim Shiau[1] and Catherine Smith[2]

[1] Lecturer, Faculty of Engineering and Surveying
University of Southern Queensland, QLD, 4350, Australia
jim.shiau@usq.edu.au

[2] Research Assistant, Faculty of Engineering and Surveying
University of Southern Queensland, QLD, 4350, Australia
catherine.smith@usq.edu.au

Keywords: earth pressure, passive resistance, retaining wall, numerical analysis, Flac.

Abstract: *Elasto-plastic analysis for classical lateral earth pressures is presented in this paper using the explicit finite difference method of FLAC. The developed numerical model consists of a rigid structure for the gravity wall, a zero thickness interface for modelling the sliding and separation between the wall and the backfill soil, and a Mohr-Coulomb soil model for the backfill. The rigid wall was pushed into the backfill soil to induce passive failure and the ultimate load required for the failure is calculated. Numerical results are compared with other available solutions and numerical difficulties experienced in the analyses are discussed.*

1. INTRODUCTION

To date, limit equilibrium methods have often been used by practicing engineers to determine lateral earth pressures. Among these are the Rankine, Coulomb, and Log-spiral techniques. These limit equilibrium methods are based on the assumption that collapse is triggered along an assumed failure surface and that, the shear stress at every point of this surface reach a limit shear strength which is governed by soil shear strength parameters such as c (cohesion) and ϕ (friction angle). The global force equilibrium solution is then solved repeatedly in order to find the lowest load by changing the geometry of the failure surface.

An inherent limitation of the limit equilibrium method is the need to define the general shape of the failure surface in advance. A typical example of this limitation is the assumption of plane failure surface in the calculation of passive resistance using Coulomb Theory. It is well known that the assumption of plane failure surface is not reasonable for rough wall. It is particularly the case for passive walls in which, as the value of soil-wall friction increases, Coulomb Theory may give increasingly non-conservative prediction. To improve this drawback, the Log-Spiral earth pressure theory was firstly described in detail by Terzaghi (1943) and Terzaghi et al. (1996). Based on the Log–Spiral method, tables and charts of passive pressure coefficients were produced for cohesionless soil and simple geometry condition (Caquot and Kerisel, 1948).

More recently, a novel numerical limit analysis using classical upper and lower bound theorems have been performed for passive earth pressure problems (Shiau et al. 2004 and 2006). Using an associated flow rule, their results typically bracket the true solution within 10% or better. The numerical techniques, developed at Newcastle, have also been successfully applied to a large number of geotechnical stability problems (Lyamin and Sloan, 2002a and 2002b).

In this paper, the classical passive earth pressure problems are investigated by using the explicit finite difference code FLAC – a popular numerical tool in Australia and many other countries. A number of modelling issues in creating an accurate model are discussed. It is hoped that this knowledge will enable some numerical pitfalls to be avoided by practicing engineers in their future analysis.

2. STATEMENT OF THE PROBLEM

The numerical experiment presented in this paper consists of a vertical gravity wall and a level backfill, as illustrated in Figure 1. The backfill soil is taken to be c - ϕ Mohr-Coulomb material with a unit weight γ. The soil-wall interface roughness is represented by a friction angle δ and an adhesion c_a. For a c- ϕ backfill, $\delta = 0$ and $c_a = 0$ indicates a perfectly smooth wall while a perfectly rough wall is modelled by adopting $\delta = \phi$ and $c_a = c$.

In a similar manner to the bearing capacity equation of Terzaghi, the total passive thrust acting on the wall, P_p, can be defined in terms of passive earth pressure coefficients $K_{p\gamma}$ and K_{pc}, according to Equation (1):

$$P_p = \frac{1}{2}\gamma H^2 K_{pr} + cHK_{pc} \tag{1}$$

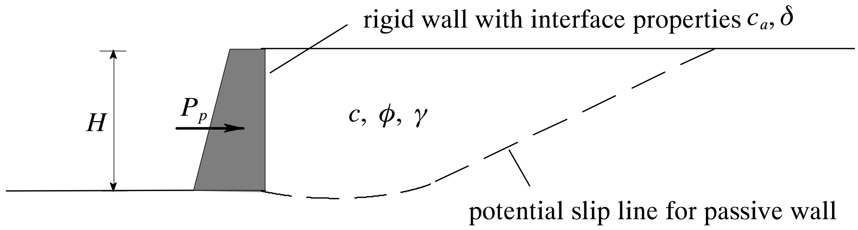

Figure 1. Problem notation and potential failure mechanism

For a cohesionless backfill soil, Equation (1) is reduced to $P_p = \frac{1}{2}\gamma H^2 K_{pr}$ and is governed by the soil-wall friction angle δ and the backfill frictional angle ϕ for a drained analysis. Using equation (1), the values of $K_{p\gamma}$ can be determined and compared with other available solutions. To determine the value of K_{pc}, a weightless soil can be given in the analysis by setting $\gamma = 0$.

In all computations presented, a cohesionless backfill soil is assumed ($c = 0$) and thus $K_{p\gamma}$ is the only coefficient presented throughout this paper. Both associated flow rule and non-associated flow rules will be examined in this paper.

3. EXPLICIT FINITE DIFFERENCE METHOD (FLAC) AND THE NUMERICAL MODEL

FLAC is a very popular tool in the design of many geotechnical structures by practising engineers in Australia and many other countries. Although the code is based on the the explicit finite difference method, it is not very different from a nonlinear finite element program. An explicit time marching scheme (known as dynamic relaxation using the full dynamic equation of motion, Otter et al. 1966) is adopted to solve the resulting equations which are identical to those in the finite element formulation. To solve a static system using the dynamic equation of motion, an artificial nodal damping is needed so that kinetic energy can be gradually removed.

Nodal unbalanced force is one of the main convergence criteria in this explicit method. In order to minimise the initial oscillation of the system, small time stepping must be used. This unavoidably increases the solution time to a certain extent. This also requires significant experience and judgement when using this numerical code. For example, the analysis in this paper requires applying a uniform velocity into the gravity wall so that a passive failure can be estimated. In practice, the method would thus suggest a small velocity to be applied to the system with a large number of time steps, thereby implying that the user would have to decide whether sufficient time steps have been performed so that a solution close to failure obtained. However, the method avoids the solution of large sets of equations (unlike the traditional finite element method) – a big saving for computer memory. Indeed, FLAC is comparable to a constant stress triangular element in the finite element method despite the difference in solution scheme.

Figure 2 shows a typical mesh for the problem considered. The bottom and right hand edges of the mesh are fixed since it is assumed that the failure mechanism is contained within the proposed grid. Note that this condition needs to be checked for each case and in some instances (e.g. for very rough soil-wall interfaces) larger meshes are necessary to ensure that the optimal failure mechanism is captured correctly. In all computations conducted, the right hand boundary is taken to be five times the height of the wall.

An elastic material is assigned to the zones of the gravity wall while the backfill soil follows a Mohr–Coulomb behaviour with either associated or non-associated flow rule. To model the effect of sliding and/or separation on the soil-structure interface, a zero thickness interface is used. Those nodes on the interface boundary are given a different material property from the one adopted for the backfill soil. For cohesionless soil, a smooth wall is modelled by adopting a zero interface friction angle δ. For a perfectly rough wall, the maximum value of wall friction δ is equal to the backfill soil friction angle ϕ. Note that the nodes at the bottom of the wall actually have no contact with the soil even though they have the same nodal coordinates. These nodes are not allowed to move in the vertical direction in order to simulate a heavy gravity wall.

To induce passive failure, a rigid retaining wall of height H is pushed horizontally into the soil. Physically this means that a small velocity should be applied to the right of the nodes that are fixed in x and y direction at the edge of gravity wall. After the resulting problem is solved for the imposed boundary conditions, the passive force P_p is obtained by adding up all the reaction forces along the nodes at the edge of gravity wall. The relevant passive earth pressure coefficients $K_{p\gamma}$ can then be found by direct substitution in Equation (1) .

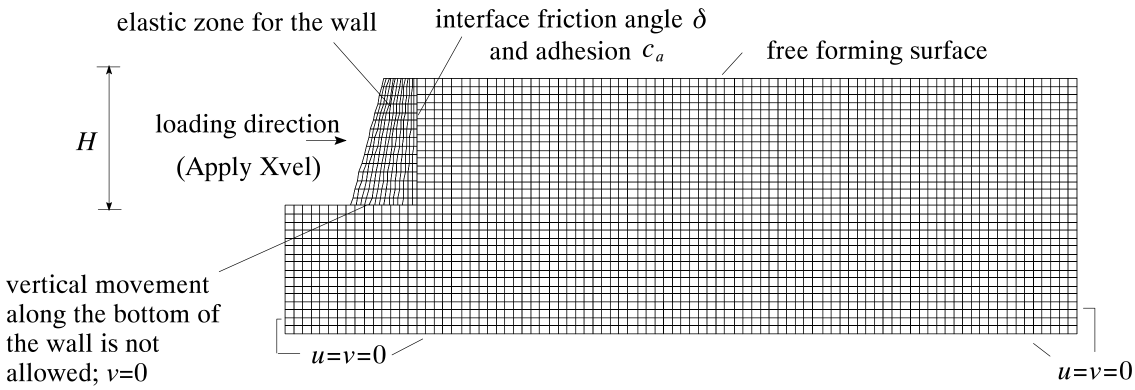

Figure 2. A typical finite difference grid for the soil-structure interaction analysis

4. RESULTS AND DISCUSSION

4.1 Model Verification

The numerical model is firstly verified with the available solution using a smooth soil–wall interface and a cohesionless backfill sand ($\phi = 40^\circ$, $c = 0$). Presented in Figure 3 are contour plots for comparing the maximum shear strain rate for two boundary conditions using an associated flow rule. The first boundary condition (FIX) represents the case where the nodes located along Side A are fixed, while the second boundary condition is for NO FIX. Figure 3 demonstrates that a better strain distribution can be obtained for the FIX condition even though both cases yield similar failure mechanisms. Note that a large stress concentration is observed near the corner of the wall with NO FIX condition. The FIX and NO FIX models predict values of $K_{p\gamma} = 5.047$ and $K_{p\gamma} = 4.928$ respectively. For this particular case ($\phi = 40^\circ$, $c = 0$), Rankine's solution gives a value of $K_{p\gamma} = 4.6$, indicating that our numerical model predicts a $K_{p\gamma}$ value that is approximately 8% greater than the true solution. A deformed grid for the NO FIX case is also shown in Figure 4, which clearly shows a shear band with a width of approximately four elements.

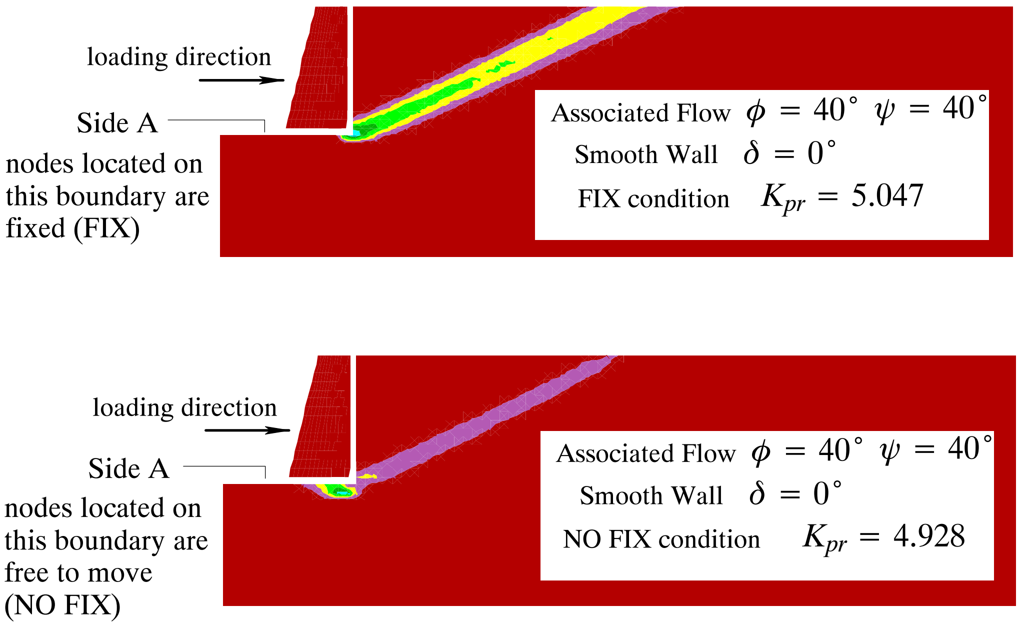

Figure 3. A comparison of maximum shear strain rate between FIX and NO FIX cases

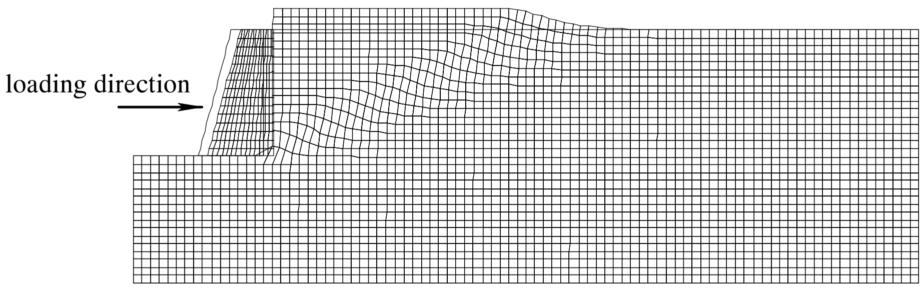

Figure 4. A deformed mesh for the NO FIX case in Figure 3

To improve solution accuracy, the total number of elements adopted in Figure 2 are doubled and a $K_{p\gamma}$ value of 4.911 for the finer mesh (not shown in this paper) is calculated. It is thus concluded that the solution can only be slightly improved by increasing the total number of elements. A fan-shaped mesh centred about the bottom corner of the retaining wall has been shown to improve the results considerably in their upper and lower limit analyses (Shiau et al. 2004 and 2006). This has the advantage of aligning stress discontinuities along the potential slip plane and can be adopted in future analyses. Langen and Vermeer (1991) have also shown that the introduction of an internal interface (near the singular plasticity point) in the finite element mesh would improve the computational results considerably. Intuitionally, the introduction of a 45 degree edge cut (Figure 5) would also benefit the numerical solution.

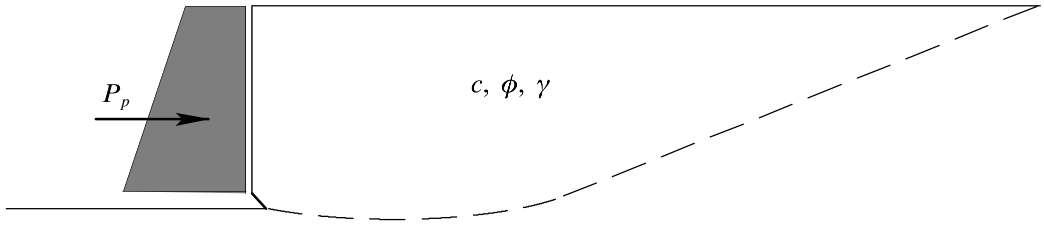

Figure 5. A proposed 45 degree edge cut near the singular point

4.2 Associated and Non-Associated Flow

Classical limit equilibrium method and limit analysis theory assume an associated flow rule, which restricts the direction of plastic flow such that $\psi = \phi$. For non-associated materials, the dilation angle ψ cannot be greater than the soil friction angle ϕ, whilst in real soils it is always smaller than ϕ. Normality is sometimes presented as a serious restriction on the use of these methods for geotechnical stability problems. Provided that the problem is not kinematically restricted, this concern is of minor importance (Davis 1968), although it is possible to carry out an analysis using a "residual" friction angle to model non-associated behaviour (Drescher and Detournay 1993, Shiau et al. 2003).

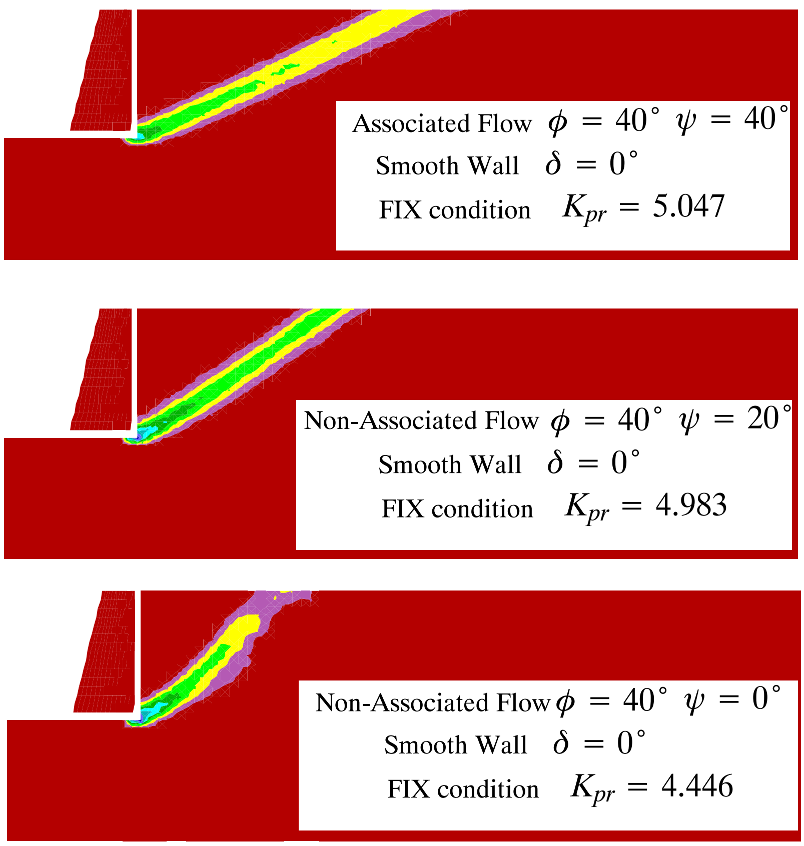

Figure 6. A comparison of maximum shear strain rate for different dilation angles (FIX)

Using the model verified above (FIX), numerical computations are conducted for non-associated flow with different dilation angles. Shown in Figure 6 is a comparison of maximum shear strain rate for different dilation angles ($\psi = 0^\circ$, 20°, and 40°). It indicates that the use of associated flow over-estimates the passive earth resistance, as in reality the dilation angle would range between zero and the internal soil friction angle.

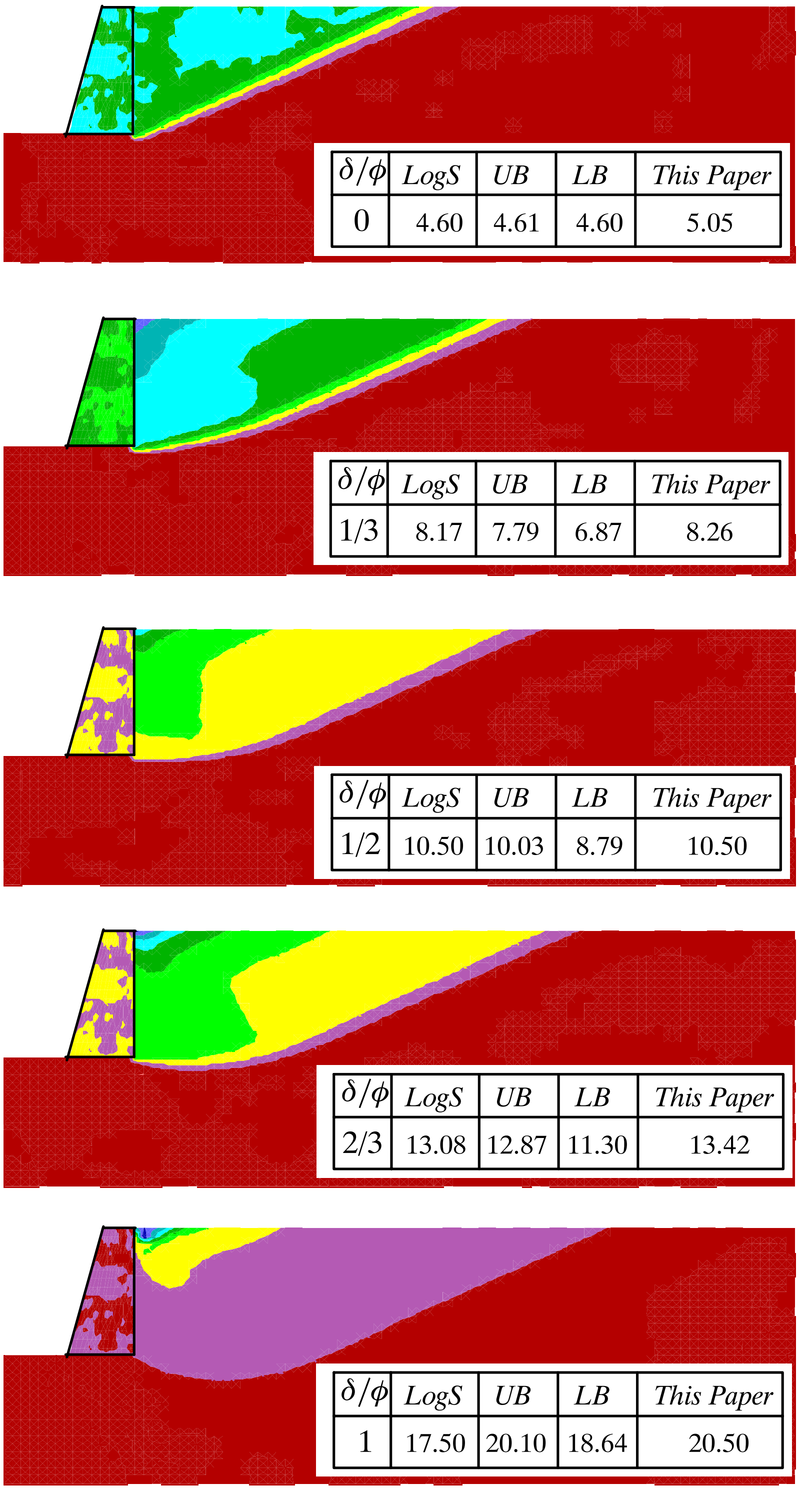

δ/ϕ	*LogS*	*UB*	*LB*	*This Paper*
0	4.60	4.61	4.60	5.05

δ/ϕ	*LogS*	*UB*	*LB*	*This Paper*
1/3	8.17	7.79	6.87	8.26

δ/ϕ	*LogS*	*UB*	*LB*	*This Paper*
1/2	10.50	10.03	8.79	10.50

δ/ϕ	*LogS*	*UB*	*LB*	*This Paper*
2/3	13.08	12.87	11.30	13.42

δ/ϕ	*LogS*	*UB*	*LB*	*This Paper*
1	17.50	20.10	18.64	20.50

Note: *LogS, UB* and *LB* are log-spiral, upper bound and lower bound results

Figure 7. Velocity contours for various wall frictions (associated flow)

4.3 Soil-Wall Interface Friction

To compare the numerical results for various soil-wall interface frictions to those using rigorous upper and lower bounds (Shiau et al. 2004 and 2006), the associated flow with soil parameters $\phi = 40^\circ$, $\psi = 40^\circ$, and $\delta/\phi = 0$, $1/3$, $1/2$, $2/3$, and 1 is adopted. Figure 7 shows the velocity diagrams (in contour format) for the comparison. Also shown in this figure are the $K_{p\gamma}$ values for the Log-Spiral method, Upper Bound, Lower Bound and FLAC.

Numerical results shown in Figure 7 predict reasonable $K_{p\gamma}$ values for all rough wall cases. For the smooth case, a value of $K_{p\gamma} = 5.05$ that is 8% higher than the true solution of $K_{p\gamma} = 4.60$ is obtained. It is interesting to note that numerical results obtained using FLAC are neither upper bound nor lower bound on the true solution. When a decision has to be made with regard to the final ultimate passive resistance for design purposes, it seems that the bounding results presented in Shiau et al. (2004 and 2006) are more reliable as the users would have a knowledge of the range of true solutions.

5. CONCLUSIONS

A numerical study on classical ultimate passive earth pressure problem has been carried out in this paper using a numerical tool called FLAC. The study covers a wide range of factors including the boundary effect, associated and non-associated flow rule, and the effect of soil-wall friction. Numerical results are compared with those using rigorous upper and lower bounds. It is concluded that reasonable predictions can be made using this numerical tool, provided that careful verification is made. The upper and lower bound results produced by Shiau et al. (2004 and 2006) are helpful in verifying the current numerical model. It would be interesting to see more results published in the future using this model.

REFERENCES

[1] Caquot, A. and Kerisel, J. (1948). *Tables for the calculation of passive pressure, active pressure and bearing capacity of foundations*, Gauthier-Villars, Paris.

[2] Davis, E. H. (1968). "Theories of plasticity and the failure of soil masses." *Soil mechanics: selected topics*. I. K. Lee. Ed., Butterworth, London. England. 341-380.

[3] Drescher, A. and Detournay, E. (1993). "Limit load in translational failure mechanisms for associative and non-associative materials." *Geotechnique*, 43(3), 443-456.

[4] Duncan, J. M and Mokwa, R. (2001). "Passive earth pressures: theories and tests." *Journal of Geotechnical and Geoenvironmental Engineering, ASCE*, 127(3), 248-257.

[5] Itasca Consulting Group (2003). *FLAC, Fast Lagrangian Analysis of Continua, Version 4.0*, Itasca Consulting Group, Minneapolis, Minnesota, USA.

[6] Langen, H. Van and Vermeer P. A. (1991). "Interface elements for singular plasticity points." *International Journal for Numerical and Analytical Methods in Geomechanics*, 15, 301-315.

[7] Lee, I. K. and Herrington J. R. (1972). "A theoretical study of the pressures acting on a rigid wall by a sloping earth or rock fill." *Geotechnique,* 22(1), 1-26.

[8] Lyamin, A. V. and Sloan, S. W. (2002a). "Lower bound limit analysis using nonlinear programming." *International Journal for Numerical Methods in Engineering,* 55, 573-611.

[9] Lyamin, A. V. and Sloan, S. W. (2002b). "Upper bound limit analysis using linear finite elements and nonlinear programming." *International Journal for Numerical and Analytical Methods in Geomechanics* , 26, 181–216.

[10] Otter, J.R.H., Cassell, A. C. and Hobbs, R. E. (1966). Dynamic relaxation (Paper No. 6986). *Proc. Inst. Civil Eng.* 35, 633–656.

[11] Shiau, J. S., Lyamin, A. V. and Sloan, S. W. (2003). "Bearing capacity of a sand layer on clay by finite element limit analysis." *Canadian Geotechnical Journal*, 40, 900–915.

[12] Shiau, J. S., Lyamin, A. V. and Sloan, S. W. (2004). "Rigorous solutions of classical lateral earth pressures." *6th Young Geotechnical Professionals Conference, Gold Coast, Australia*, 162–167.

[13] Shiau, J. S., Augarde, C. E., Lyamin, A. V. and Sloan, S. W. (2006). "Passive earth resistance in cohesionless soil." *Canadian Geotechnical Journal*. (Accepted)

[14] Shiau, J. S., Merifield, R. S., Lyamin, A. V. and Sloan, S. W. (2006). "Undrained stability of footings on slopes." *Journal of Geotechnical and Geoenvironmental Engineering, ASCE*. (Accepted)

[15] Terzaghi, K. (1943). *Theoretical soil mechanics*, John Wiley and Sons, Inc., New York.

[16] Terzaghi, K., Peck, R. B., and Mezri, G. (1996). *Soil mechanics in engineering practice*, 3rd Ed., John Wiley and Sons, Inc., New York.